Characteristics and Changes in Air Temperature and Glacier's Response on the North Slope of Mt. Qomolangma (Mt. Everest)

Authors: Yang, Xingguo, Zhang, Tingjun, Qin, Dahe, Kang, Shichang, and Qin, Xiang

Source: Arctic, Antarctic, and Alpine Research, 43(1) : 147-160

Published By: Institute of Arctic and Alpine Research (INSTAAR), University of Colorado

URL: https://doi.org/10.1657/1938-4246-43.1.147

Arctic, Antarctic, and Alpine Research, Vol. 43, No. 1, 2011, pp. 147–160

Characteristics and Changes in Air Temperature and Glacier's Response on the North Slope of Mt. Qomolangma (Mt. Everest)

*Xingguo Yang**
Tingjun Zhang†‡#*
*Dahe Qin**
*Shichang Kang**§ *and*
*Xiang Qin**

*State Key Laboratory of Cryospheric Sciences, Cold and Arid Regions Environmental and Engineering Research Institute, Chinese Academy of Sciences, Lanzhou 730000, China
†State Key Laboratory of Frozen Soil Engineering, Cold and Arid Regions Environmental and Engineering Research Institute, Chinese Academy of Sciences, Lanzhou 730000, China
‡National Snow and Ice Data Center, Cooperative Institute for Research in Environmental Sciences, University of Colorado, Boulder, Colorado 80309, U.S.A.
§Institute of Tibetan Plateau Research, Chinese Academy of Sciences, Beijing 100085, China
#Corresponding author: National Snow and Ice Data Center, Cooperative Institute for Research in Environmental Sciences, University of Colorado, Boulder, Colorado 80309, U.S.A.
tzhang@nsidc.org

Abstract

Weather and climatic conditions over the Himalaya regions are of great interest to the scientific community at large. The objective of this study is to present spatial and temporal variations of air temperatures and relative humidity on the north slope of Mt. Qomolangma. Both hourly air temperatures and relative humidity were measured at seven automatic weather stations (AWS) from 5207 to 7028 m a.s.l. from May 2007 through September 2008. Long-term (1959–2007) air temperature and precipitation data were obtained from Dingri Meteorological Station. The preliminary results show that the elevational gradient of mean annual air temperature is non-linear, which decreases from 0.2 °C at an elevation of 5207 m to −4.4 °C at 5792 m, and −5.4 °C at 5955 m. The maxima are 14.6, 9.1, and 18.6 °C, and the minima are −24.2, −28.8, and −29.3 °C at the three elevations, respectively. The relative humidity does not change significantly with increasing elevation except over glacier ice, but the mixing ratio decreases due to the decrease in air temperature. The mean diurnal ranges of air temperature and relative humidity decrease with increasing elevation. The daily maximum air temperature occurs significantly later at the high-elevation site than that at the low elevation site because the air temperature at the high-elevation site is affected to a large extent by downward mixing of warm air near the ablation zone of the glacier during daytime. The air moisture content reflects the pronounced alternation of the wet and dry seasons, and the highest water vapor content is associated with the southwesterly Indian monsoon. The mean annual surface air temperature–elevation gradient is 0.72 ± 0.01 °C (100 m)$^{-1}$, and also shows a pronounced seasonal signature. Mean annual air temperatures have increased by about 0.62 °C per decade over the last 49 years in this region; the greatest warming trend is observed in winter, the smallest in summer. Warmer conditions have been observed since the mid-1980s. Additional studies have shown a reduction in precipitation in the 1960s that resulted in a decrease in net snow accumulation. Therefore, accelerated retreat of the Rongbuk Glacier since the 1980s may be caused by rising air temperature and the decreased precipitation.

DOI: 10.1657/1938-4246-43.1.147

Introduction

Mountain systems cover about one-fifth of the earth's continental areas and are all inhabited to a greater or lesser extent except Antarctica. Mountains represent unique areas for the detection of climatic change and the assessment of climate-related impacts (Beniston, 2003). Concerns have been expressed by the scientific community that climatic changes will severely impact the mountain regions of the world because high-elevation areas seem to be warming more, and perhaps faster than the rest of the globe. Future climate change associated with global warming is likely to be amplified in mountain regions (Barry, 1992, 2008; Aizen et al., 1997; Beniston et al., 1997; Diaz and Bradley, 1997; Giorgi et al., 1997; Liu and Chen, 2000; Beniston, 2003). One of the most clear and potentially severe impacts is likely to be the retreat and, in some cases, disappearance of many alpine glaciers throughout the world. It is estimated that sea level rise due to melting of alpine glaciers and icecaps was 0.50 ± 0.18 mm a^{-1} between 1961 and 2004 (IPCC, 2007a). This contribution has increased to 0.77 ± 0.26 mm a^{-1}, accounting for approximately 20–30% of a recent estimate of 3.2 ± 0.4 mm a^{-1} of total sea-level rise for 1993–2005 (Kaser et al., 2006). Estimates of additional sea-level rise due to alpine glacier and ice cap melt range from 0.046–0.051 m (Raper and Braithwaite, 2006) to 0.1–0.25 m (Meier et al., 2007) by 2100. The other likely impact of climate change on mountains is associated with biodiversity, ecosystems, hydrologic systems, permafrost conditions, and landscape of high mountain environments (Diaz and Bradley, 1997; Giorgi et al., 1997; Zhang, 2007). Therefore, observational studies of change in high-elevation areas are becoming important both to detect climate change (Giorgi et al., 1997) and to provide basic data for many other research fields (Rolland, 2003). Unfortunately, long-term and systematic *in situ* measurements are often sparse in mountainous areas (Richardson et al., 2004), especially at high elevations or in uninhabited areas (Rolland, 2003), due mainly to the difficulty of installing and maintaining meteorological instruments. Thus, obtaining precise meteorological and climatic data in mountainous areas is difficult (Beniston et al., 1997).

1523-0430/11 $7.00

The Himalaya in central Asia is a 2500-km-long, 250- to 400-km-wide range that extends from 34–36°N, 74°E in the northwest to 27–28°N, 95°E in the east. It has a total glacier area of about 35,110 km^2, with an estimated total ice volume of 3700 km^3 (Qin, 1999). It is well recognized that the Himalaya significantly affects the climate and environmental systems of China and Asia (Ye and Gao, 1979), and in some cases, could affect global atmospheric circulation patterns (Jenkins et al., 1987; Yanai and Li, 1994; Barry, 2008). Various studies suggest that warming in the Himalaya has been much greater than the global average of 0.74 °C over the last 100 years (Du et al., 2004; IPCC, 2007b). Glaciers in the Himalaya are retreating faster than the world average and are thinning by 0.3–1 m a^{-1} (Dyurgerov and Meier, 2005). Nevertheless, very little long-term and systemic monitoring of climatic variables has been undertaken in this extraordinarily heterogeneous mountain topography, particularly for those regions higher than 4000 m a.s.l. (Rees and Collins, 2006), such as Mt. Qomolangma (27°59′N, 86°55′E, 8844.43 m a.s.l.) in the central Himalaya, the highest peak on Earth. Due to its unique natural ecology and geographical conditions, this region is extremely sensitive to climate and environmental change (Liu and Chen, 2000) and provides favorable conditions for glacier development (Shi, 2008). Glaciers occupy a total surface area of about 1600 km^2, approximately 32% of the entire Mt. Qomolangma region (Shi, 2004).

Sporadic historical measurements of meteorological variables extend back to the 1920s. Somervell and Whipple (1926) conducted some measurements of air temperature, wind direction, and speed, and related weather conditions at five different elevations of the north slope of Mt. Qomolangma in April and May, 1924. Since the late 1950s, three major comprehensive scientific expeditions were conducted in this region during the periods 1959–1960, 1966–1968, and 1975, focusing on meteorology, glaciology, hydrology, geology, and so on (Xie 1975; Shen, 1975; Gao, 1980). Later, some studies were performed by individuals (Jenkins et al., 1987; Kang et al., 2001; Cai et al., 2007; Zou et al., 2008). Since the 1990s, the "Pyramid" meteorological observatory, a portable weather station and the world's highest ground automatic weather station (AWS), was installed on the south side of Mt. Qomolangma at 5050, 7986, and 8000 m a.s.l. in 1993, 1998, and 2008, respectively, to collect meteorological data from the summit region (Bertolani and Bollasina, 2000; Moore and Semple, 2004). To date, systematic and continuous meteorological measurements are very limited on the north slope of Mt. Qomolangma due to its high elevation, harsh environmental conditions, and difficult access.

In order to comprehensively understand meteorological conditions and monitor climate change on the north slope of Mt. Qomolangma, seven AWSs were established in May 2007 and made measurements until September 2008. This paper demonstrates the characteristics of the air temperature and relative humidity in the study region using *in situ* measurements from these seven AWSs located from 5207 to 7028 m a.s.l. (Fig. 1). We further investigate the long-term (1959–2007) changes in air temperature and glacier response using data from the Dingri meteorological station (4301 m a.s.l.).

Experimental Setup

Figure 1 illustrates the relief, terrain, glacier distribution, and the seven observational sites on the north slope of Mt. Qomolangma. There are four main parts of the Rongbuk Glacier—the West, Middle, East, and Far East Rongbuk Glacier—with a total surface area of about 148 km^2 (Shi, 2004). Two tributary glaciers, the West Rongbuk and the Middle Rongbuk, converge to form the tongue-like Rongbuk Glacier extending into the Rongbuk Valley, which is oriented from north-northwest to south-southeast, with a floor width of 1000–1500 m. The East and Far East Rongbuk Glaciers are oriented from southeast to northwest and east to west, respectively (Shi, 2004). The remaining Rongbuk Valley surface is covered by multi-sized rocks and moraines.

Generally, local weather is controlled mainly by the low-level southwesterly Indian monsoon regime from June through September, overlain by tropical easterlies (Ye and Gao, 1979; Barry, 2008). From October through May, the region is just north of the axis of the subtropical westerly jet stream in the upper troposphere (Ye and Gao, 1979). The winds come from west to the east and cause gales and blizzards over the ridges and peaks. These westerly winds decrease substantially in late May. There is a transition period in the upper troposphere between the easterly winds and the re-establishment of the westerlies by the end of September, and persistent strong winds can be expected in this area (Ye and Gao, 1979; Barry, 2008).

Seven sites were established along the traditional mountaineering line on the north slope of Mt. Qomolangma (Fig. 1). These sites cover a range of elevation of 1800 m (Table 1). Site 1 is located in the middle of the Rongbuk Valley and about 2 km from the Middle Rongbuk Glacier terminus. There are several sporadic supra-glacial lakes with a total area of about 0.8 km^2 between site 1 and the glacier terminus. Site 2 is located in the East Rongbuk Valley about 1500 m from the East Rongbuk Glacier terminus. Sites 3 and 4 are situated on the lateral moraine of the East Rongbuk Glacier, close to areas of seracs 10–20 m high. Site 5 is on the southeast-facing slope covered by rock debris and 30 m upstream of the East Rongbuk Glacier. Site 6 is situated on the Ruopula Pass, which is the accumulation zone of the East Rongbuk Glacier. On both the south and north sides of site 6 are open areas. The mountains to the east and west of site 6 are covered by snow and firn. Site 7 is on the west side of the North Hill, which is oriented from north to south. The surface is covered by snow and firn. More details for each site are given in Table 1. To aid in understanding the environment, Figure 2 shows the different surface conditions and environments for sites 1, 3, 4, and 6.

Air temperature and relative humidity were measured with a humidity and temperature probe HMP45D and installed at 2 m above the surface and shielded by a solar radiation shield with natural ventilation. A Young anemometer (05103) was installed at the same height as the humidity and temperature probe. Atmospheric pressure was measured with a pressure sensor and installed in the data logger box at 0.5 m height. Measurements, including mean, maximum, and minimum values, were recorded every hour. Technical details about the sensors are given in Table 2. Before activation, all sensors were calibrated. Power for the AWSs was supplied by solar panels in combination with batteries. There were some missing values for sites 2, 5, 6, and 7 due to power and AWS malfunction during the period of measurements (Table 1).

The local time is 2 hours and 14 minutes behind Beijing Standard Time. In this article, all times are given as Beijing Standard Time (BT). Daily air temperature and rainfall data from the Dingri Meteorological Station from 1959 to 2008 are also used in this study. Dingri (20°38′N, 87°05′E, 4301 m a.s.l.) is about 60 km northeast of Mt. Qomolangma.

Using hourly air temperatures, we also estimated the surface air temperature–elevation gradients between two neighboring stations. Daily surface air temperature–elevation gradients are

FIGURE 1. Geographical location of Mt. Qomolangma region in southwestern China (up left corner) with major mountain peaks. Automatic weather stations (AWSs) are located along the traditional mountaineering line on the north slope of Mt. Qomolangma.

an average of hourly surface air temperature–elevation gradients, while monthly and annual surface air temperature–elevation gradients are estimated directly using daily surface air temperature–elevation gradients. The error bars for monthly and annual surface air temperature–elevation gradients are one standard deviation from their means, respectively.

Results

ALTITUDINAL VARIABILITY

Daily maximum, mean, and minimum air temperatures decrease with increasing elevation from site 1 to 7, with the exception of maximum air temperatures at site 4 from May to

TABLE 1

Summaries for seven sites, measurement of meteorological factors, and available data on the north slope of Mt. Qomolangma.

Site No.	Latitude (N)	Longitude (E)	Altitude (m a.s.l.)	Site Description	Variables measured [a]	Observational period
1 [b]	28°8′	86°51′	5207	multi-sized stones flat surface	T, H, d, u, p, R, W, S	5 May 2007 to 31 Aug. 2008
2 [c]	28°6′	86°53′	5550	multi-sized stones flat surface	T, H, d, u, p	5 May 2007 to 30 May 2008
3	28°5′	86°55′	5792	moraine 4°incline	T, H, d, u, p	5 May 2007 to 31 Aug. 2008
4 [d]	28°4′	86°55′	5955	moraine near ice 6° incline	T, H, d, u, p	5 May 2007 to 31 Jul. 2008
5	28°2′	86°56′	6300	rock debris 10° incline	T, H, d, u, p	Apr. 20 to 8 May 2008
6	28°1′	86°57′	6560	snow/firn flat surface	T, H, d, u, p, R_1	2 Oct. 2007 to 19 Jan. 2008
7 [e]	28°0′	86°55′	7028	snow/firn 15° incline	T, d, u, p [e]	26 Apr. to 30 Sep. 2007

a: d, wind direction; H, relative humidity; p, atmospheric pressure; R, radiation; S, sounding; T, air temperature; u, wind speed; W, weather reports.

b: W only was recorded from 10 April to 8 May 2007 and 13 April to 8 May 2008 at base camp. S was carried out two times (7:00 and 19:00 BT) every day during the same period with the exception of 6, 7, 8, and 9 May 2007; and 22 and 23 April, and 6, 7, and 8 May 2008, when S was operated at a frequency of 6 to 12 times a day.

c: data absent from 1 November 2007 to 25 April 2008 and T and H were available only in May 2008.

d: data absent from 1 to 30 June 2007, and u and d were not available from 1 January to 30 July 2008.

e: data were recorded every two hours.

September (Fig. 3, Table 3). Maximum air temperatures are higher at site 4 than at site 3 during this period. This may be the result of the special position of site 4, which is on a south facing moraine slope and can receive more solar radiation when the intensity of incoming shortwave radiation is high from May to September. A detailed comparison of the mean, maximum, and minimum air temperature profiles from Dingri meteorological station to site 6 is shown in Figure 4. There is a rapid change in air temperatures from the moraine and ice field at site 3 to the ice field at site 6 due to differences in surface conditions (see Table 1).

Surface air temperature–elevation gradients show variability with shallower regions around 5207 m a.s.l. and 5955 m a.s.l. and a steeper region toward the ice field (Fig. 4). They become steeper from sites 1 and 3 with value of 0.74 $(100\ m)^{-1}$ to sites 4 and 6 with a value of 0.84 $(100\ m)^{-1}$ during October of 2007 to January of 2008. This may be related to different surface conditions that result in the greater air temperature difference. Sites 1 and 3 were established over multi-size stones and moraine surfaces, while sites 4 and 6 had two distinct surface conditions. Site 4 had a moraine surface, while site 6 was on glacier ice (Fig. 2). Due to high albedo of ice surface, air temperature would be relatively lower at site 6 if the same measurements were conducted over a moraine surface at the same elevation, resulting a large difference in air temperature or surface air temperature–elevation gradient between sites 4 and 6. Moreover, higher wind speed may also contribute to the steeper surface air temperature–elevation gradients around site 6. It has been reported surface air temperature–elevation gradients are strongly coupled with cloud cover, sunshine duration, and synoptic conditions (Harding, 1979; Bennett, 1997; Pepin, 2001). Over the study area during October 2007 to January 2008, clouds

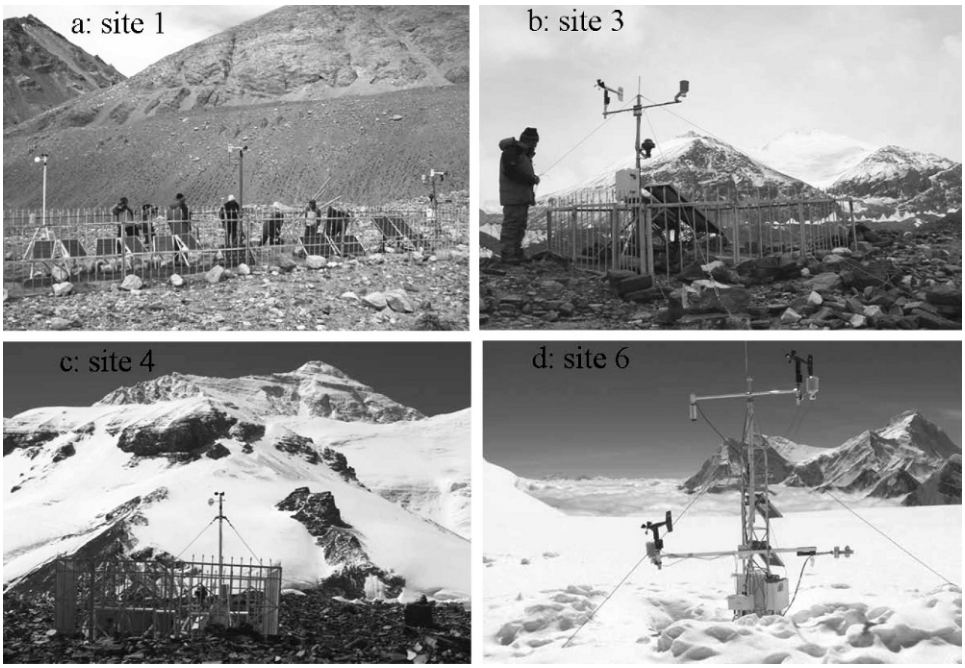

FIGURE 2. Specific site characteristics of automatic weather stations and their surrounding environments at sites 1, 3, 4, and 6.

TABLE 2

List of sensors and their specifications.

Elements (unit)	Sensor Type	Specifications
Air temperature (°C)	Vaisala HMP 45D	Accuracy : ±0.2 °C; Range: −39.2 ~ 60 °C
Relative humidity (%)	Vaisala HMP 45D	Accuracy: ±2%; Range: 0.8% ~ 100%
Wind speed (m s^{-1})	Young 05103	Accuracy: ±0.3 m s^{-1}; Range: 0 ~ 100 m s^{-1}
Wind direction (degrees)	Young 05103	Accuracy: ±3°; Range: 0° ~ 355°
Atmospheric pressure (hPa)	Vaisala PTB210	Accuracy: ±0.35 hPa; Range: 50 ~ 1100 hPa;

appeared frequently at local noon above 6000 m a.s.l. Thus, more clouds with less sunshine duration cool down the entire atmosphere under the cloud cover, resulting in steeper surface air temperature–elevation gradients at higher elevations. Pepin (2000) reported that surface air temperature–elevation gradients are also strongly dependent upon slope and aspect of mountains. The difference in surface air temperature–elevation gradients may be due to the integrated effect of factors mentioned above. However, the detailed mechanisms require further research.

As can be seen in Figure 5a, the relative humidity (RH) was essentially constant with elevation except for a positive anomaly at site 6. Mean values of RH from October 2007 through January 2008 are 23.9, 30.8, 25.3, and 36.4% at sites 1, 3, 4, and 6, respectively. The mixing ratio generally decreased with increasing elevation during the entire period of measurement (with the exception of site 4, where values of the mixing ratio are higher than at site 3), especially from late May to early October when the area was under the control of the southwesterly Indian monsoon (Fig 5b). The fact that site 6 showed somewhat higher values of RH compared to sites 1, 3, and 4 does not represent an increasing amount of air moisture since the values of mixing ratios do not show the same increase (Fig. 5b). Lower air temperature over the ice surface indeed results in higher relative humidity.

DIURNAL VARIABILITY

Mean diurnal cycles of air temperature based on hourly observations at sites 1 and 3 show different characteristics in each of the four seasons (Fig. 6). In summer (June to August), maximum mean daily air temperatures are 9.3 and 1.3 °C, with minimum daily air temperatures of 3.9 and −2.0 °C. In winter (December to February), maximum daily air temperatures are −3.1 and −10.6 °C, with minima of −9.8 and −13.9 °C. There are no pronounced differences in air temperatures at sites 1 and 3 between spring (March to May) and autumn (September to November). The standard deviations of air temperatures from their mean are smallest in summer (Fig. 6). This is because from June through early October the north slope region of Mt. Qomolangma is under control of the southwesterly Indian monsoon and cloud cover reduces the diurnal variations of air temperatures.

Maximum daily mean air temperature occurs significantly earlier in the day at site 1 than at sites 3 and 4 during the entire measuring period with the exception of winter. The reason is probably that the air temperature over the melting ice surface depends to a large extent on downward mixing of warm air, whereas the air temperature over other surfaces is dominated by local radiative heating. Therefore, the effect of radiative heating is retarded at sites 3 and 4. Other studies (Schneider, 1999; Wagnon et al., 1999, 2003; Greuell and Smeets, 2001; Reijmer and Oerlemans, 2002; Favier et al., 2004; Sicart et al., 2005) have reported that cooling dominates over the ice surface, with a downward sensible heat flux toward the ice surface. Although sites 3 and 4 are located on moraine beside the glacier, they appear to be affected by downward mixing of warm air since they are close to the ablation zone of the East Rongbuk Glacier. The fact that the time of maximum mixing ratio is later than the time of maximum air temperature at site 3 is consistent with this view, as discussed below (Fig. 7). Similar phenomena have been observed along the margin of the Greenland ice sheet in summer (Oerlemans and Vugts, 1993).

Figure 3d illustrates the diurnal range of air temperature (DRT), which is the difference between daily maximum and minimum air temperatures at different sites. The annual mean values of DRT for sites 1, 3, and 4 are listed in Table 3. Again, mean values of DRT from October 2007 through January 2008 were 10.4, 6.9, 9.7, and 5.9 °C at sites 1, 3, 4, and 6 and mean values from April through May, 2008, were 12.1, 10.9, 11.7, and 9.5 °C at sites 1, 3, 4, and 5, respectively. The mean values of DRT decrease with increasing elevation with the exception of site 4. This feature is similar to that in the Qinling Mountain of China (Tang and Fang, 2006), the Rocky Mountains of North America (Pepin, 2000), and Kilimanjaro of Tanzania (Duane et al., 2008). This decreasing trend is because the summits are exposed to upper tropospheric flow at all times and effectively experience more maritime-like conditions. This feature is different from the North Slope of Alaska, where there is a rapid increasing trend in diurnal temperature range with increasing elevation because the lower elevation region is strongly influenced by the marine environment while the higher elevation area is affected by a continental environment (Zhang et al., 1996). The relatively high value of DRT at site 4 is possibly associated with its special position, as mentioned above.

Mean daily maximum relative humidity generally appears at about daybreak, at the time of minimum temperature at sites 1, 3, and 4 due to the effect of air temperature (not shown). After sunrise, relative humidity drops rapidly and reaches a minimum at the time of maximum temperature. It rises gradually from late afternoon through night. Mean values of relative humidity from October 2007 through January 2008 show the same patterns with the exception of site 6, where maximum relative humidity appears in the afternoon. The convective clouds usually appear at site 6 during the early measurement period and may account for this observation. Additional analysis shows that the mean diurnal range of relative humidity decreases with increasing elevation, which is related to the decrease of DRT as mentioned above.

Mean diurnal cycles of mixing ratio based on hourly values show similar peaks in the late afternoon in different seasons (Fig. 7). The maximum mixing ratio generally occurs later than the time of maximum air temperature in spring, summer, and autumn at site 3 due to the retarded effect of radiative heating, as mentioned above. At site 1, values of mixing ratio are larger than those at site 3, and the time of the maximum is the same as at site 3. Yang et al. (submitted, 2010) pointed out that the annual mean of diurnal wind direction at site 1 was characterized by downslope flow (SE and SSE) from the glacier area. The mean frequency of

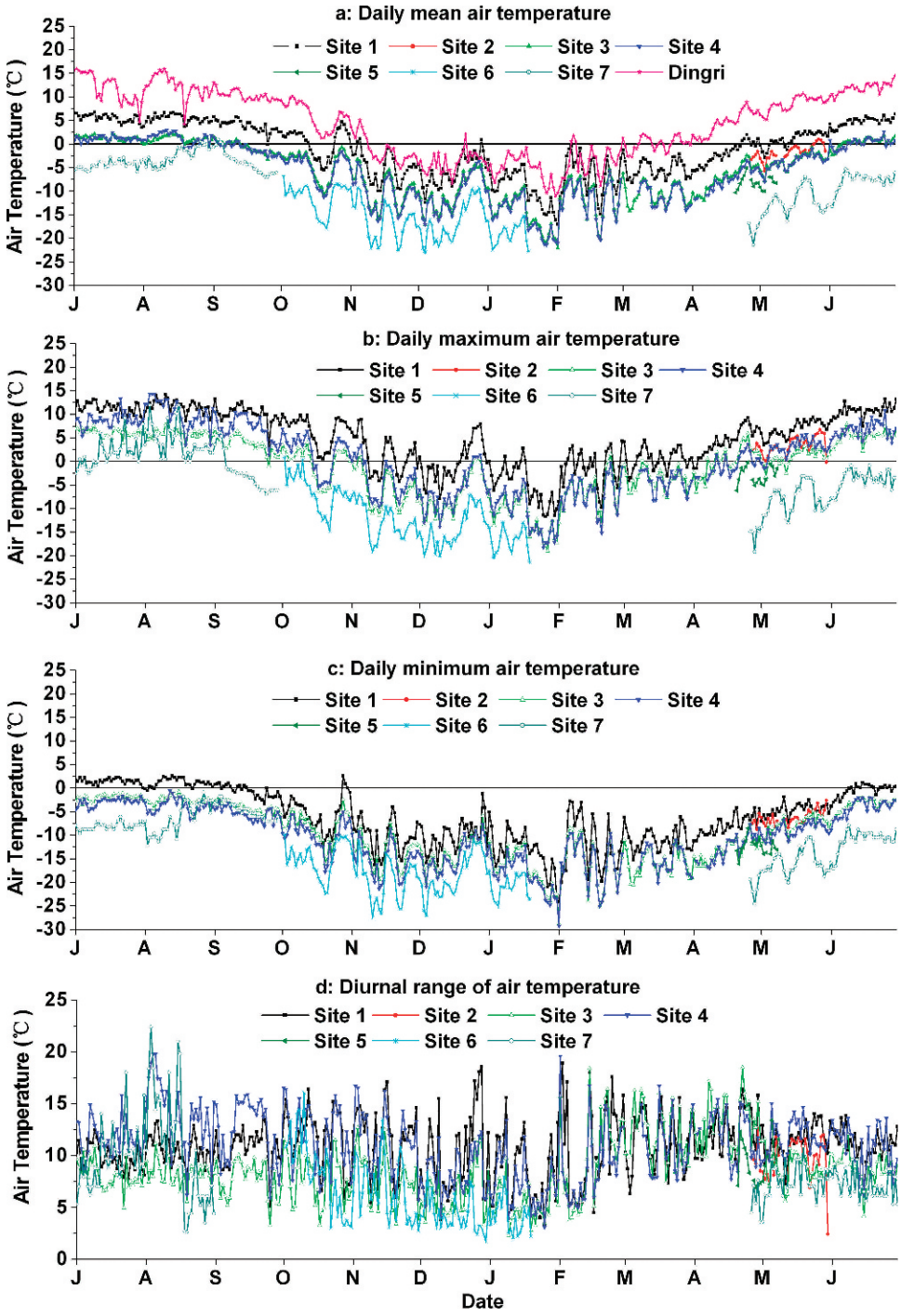

FIGURE 3. Temporal variations of daily mean (a), maximum (b), minimum (c) and diurnal range (d) of air temperatures at all sites and Dingri meteorological station. All available data are used over measuring period.

downslope winds were approximately 58.8%. The upslope (NW and NNW) wind appears mainly from 10:00 to 16:00. Therefore, the feature of the mixing ratio at site 1 can be attributed to the following effects: (1) evapotranspiration from the Rongbuk Valley surface and evaporation from sporadic supra-glacial lakes may lead to a higher mixing ratio; (2) more air moisture from the larger Rongbuk Glacier (93 km^2) brought by the glacier wind (Table 3) also contributes. These two effects require further research. The daily mean mixing ratio from October 2007 through January 2008 at sites 1, 3, 4, and 6 also shows the same features (not shown). Again, the highest mean diurnal ranges of mixing ratio occur in summer and the lowest in winter due to radiatively driven evaporation at all sites.

SEASONAL VARIABILITY

The air temperatures at all sites also show a pronounced seasonal variability, with the highest daily mean air temperatures appearing in August and the lowest in January for sites 1, 3, and 4 (Fig. 3). From June to August, daily mean air temperatures are above 0 °C at sites 3 and 4, which means glacier ablation occurs mainly during this period. The smallest monthly mean values of DRT are observed in January at site 1, 3, and 4 when solar radiation intensity is the lowest, whereas the largest values appear in April before the onset of the southwesterly Indian monsoon.

Monthly mean surface air temperature–elevation gradients, calculated using daily mean surface air temperature–elevation

TABLE 3

Meteorological variables at each site on the north slope of Mt. Qomolangma during May of 2007 to August of 2008.

Meteorological variables		Site No. 1	2*	3	4*	5*	6*	7*	Dingri
Air temperature (°C)	Average	0.2	−1.9	−4.4	−5.4	−8.3	−15.4	−8.7	5.1
	Maximum	16.4	6.7	9.1	18.6	0.2	0.8	9.2	—
	Minimum	−24.2	−8.8	−28.8	−29.3	−16.1	−27.5	−24.6	—
	Annual mean DRT	10.8	—	8.6	11.1	—	—	—	—
Surface air temperature-elevation gradient (°C (100 m^{-1}))	Average	0.62	0.71	0.80	0.67	0.74	0.84	0.60	—
Wind speed (m s^{-1})	Average	5.0	4.3	5.0	1.6	3.7	10.9	—	3.3
	Maximum	43.1	11.7	57.1	30.0	16.6	34.9	—	—
Prevailing wind direction		SE, SSE	E, ESE	NW, WNW	N, NNW	—	NW, NNW	—	—
Relative humidity (%)	Average	47.2	44.7	46.6	46.9	33.8	36.4	—	37.0
	Minimum	3.0	5.0	1.0	4.0	6.0	9.1	—	—
Mixing ratio (g kg^{-1})	Average	4.1	2.9	3.2	3.1	1.5	0.8	—	3.9
	Maximum	11.8	7.0	8.9	9.3	3.9	4.0	—	—
	Minimum	0.1	0.3	0.1	0.1	0.2	0.1	—	—

* Average, maximum, or minimum values are only calculated based on available data as shown in Table 1.

gradients at all sites, also show pronounced seasonal variations, with a range of 0.54 ± 0.11 °C (100 m)$^{-1}$ in February to 0.80 ± 0.03 °C (100 m)$^{-1}$ in April (Fig. 8). The seasonal average values of surface air temperature–elevation gradients are 0.78, 0.70, 0.74, and 0.63 °C (100 m)$^{-1}$ in spring, summer, autumn, and winter, respectively. It is primarily the low air moisture content and high wind speeds that make the surface air temperature–elevation gradients steeper in spring. High air moisture content (Fig. 5) and low wind speed may cause a shallower surface air temperature–elevation gradients during the monsoon season. The annual mean surface air temperature–elevation gradients are 0.72 ± 0.01 °C (100 m)$^{-1}$. However, these results are obtained with air temperatures from site 1 to site 7. The temporal series of air temperatures at some sites, such as site 4, 5, 6, and 7 are only from a few months, and not an entire year (see Table 1). This may lead to an estimate of the seasonal surface air temperature–elevation gradients that is different from its true value.

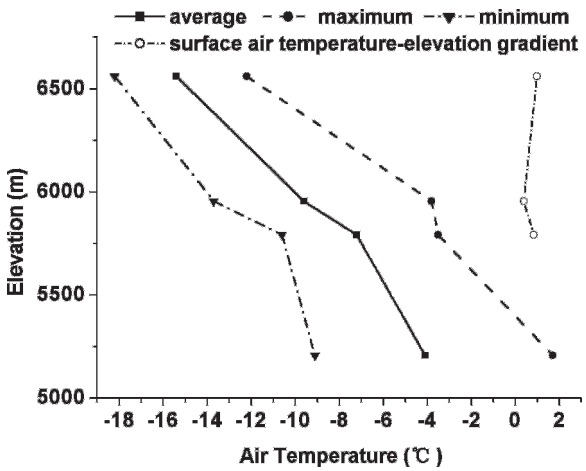

FIGURE 4. Vertical profiles of mean, maximum, and minimum air temperatures and surface air temperature–elevation gradients from site 1 to site 6. Mean, maximum, and minimum air temperatures are calculated using data from October 2007 to January 2008. Surface air temperature–elevation gradients are calculated between sites 1 and 3, sites 3 and 4, sites 4 and 6.

The annual cycle of air moisture reflects the pronounced alternation of the wet and dry seasons on the north slope of Mt. Qomolangma (Fig. 5). Air moisture content is highest from late May to early October, indicating that most of the water vapor in the north slope region of Mt. Qomolangma is brought with the southwesterly Indian monsoon. Because this is also the period of highest air temperature (Fig. 3), this may explain the occurrence of the greatest snow accumulation and the highest ablation of glaciers during summer on the north slope of Mt. Qomolangma (Fujita and Ageta, 2000).

LONG-TERM CHANGES IN AIR TEMPERATURE AND ITS EFFECT ON GLACIERS

As noted above, there has been little systematic long-term collection of meteorological records on the north slope of Mt. Qomolangma. In order to investigate the long-term changes in air temperature and glacier response, precipitation and daily mean air temperature (1959–2007) data from the Dingri meteorological station are used.

The spatial homogeneity of the air temperature regime between the north slope of Mt. Qomolangma and Dingri is identified using linear correlation analysis. Table 4 lists linear correlation coefficients (R^2) based on daily air temperature between Dingri and sites 1, 3, 4, 6, and 7. There are close linear correlations between Dingri and sites 1, 3, and 4 with R^2 above 0.80, whereas the correlation between Dingri and site 6 is relatively weak. Similarly, R^2 between site 1 and sites 3 and 4, and between site 3 and sites 4 and 6 are above 0.80, whereas the R^2 value between site 1 and 6 is reduced to 0.66 but still significant with $p < 0.05$. This suggests that air temperatures are well correlated between sites at lower elevations. The correlations between site 7 and the other sites are less pronounced with R^2 ranging from 0.15 to 0.45 and $p > 0.05$ (Table 4). The poor correlation between site 7 and other sites/station may be due to its site location as described in the section Experimental Setup. This implies air temperatures at higher elevations with ice/snow–covered surfaces are also well correlated with air temperatures at lower elevations on the north slope of Mt. Qomolangma. Therefore, long-term daily air temperatures from Dingri can in general be used to estimate

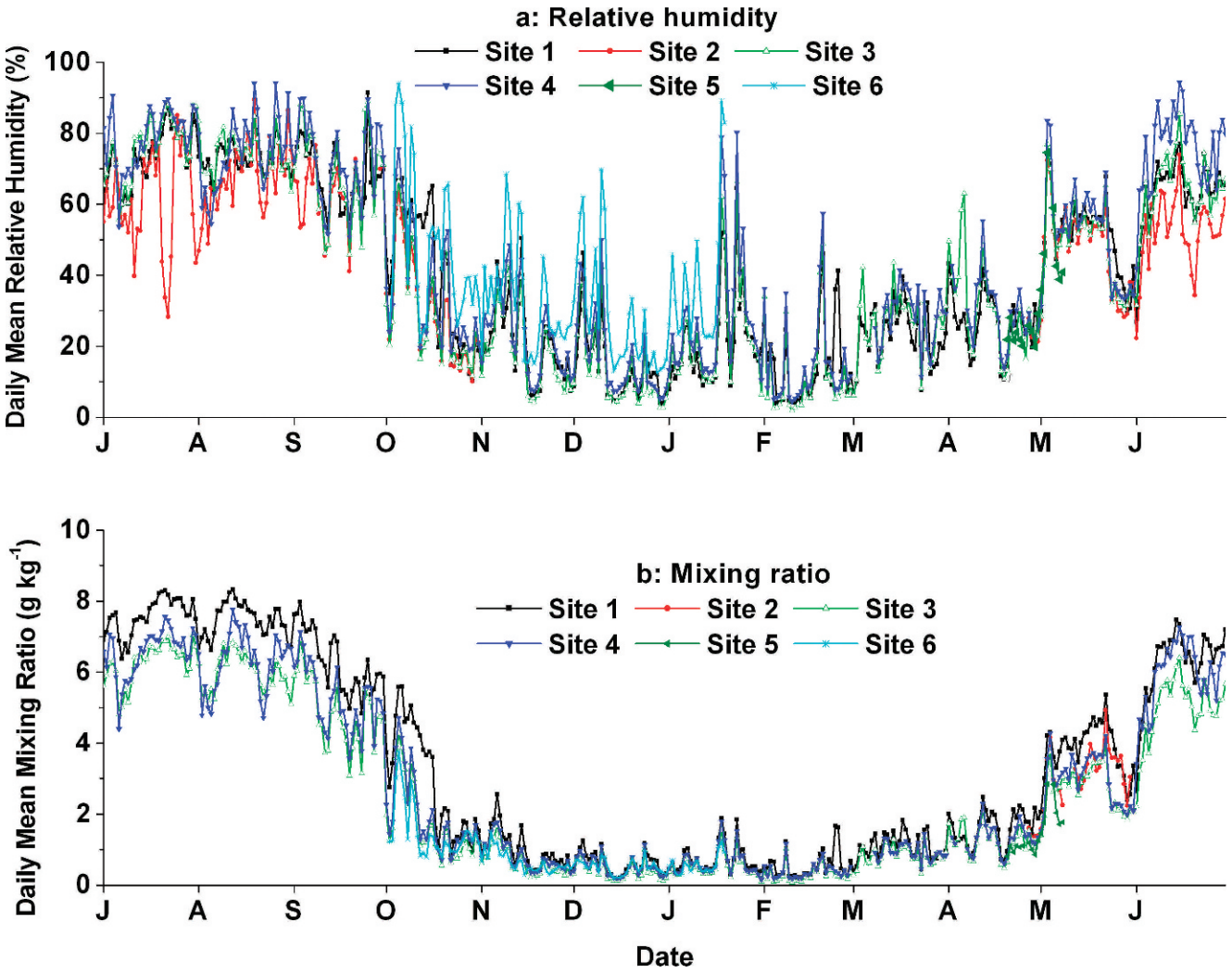

FIGURE 5. Temporal variations of relative humidity (a) and mixing ratio (b) at all sites except site 7. All available data are used over measuring period.

long-term daily air temperatures on the north slope of Mt. Qomolangma. However, it has to be noted that the *in situ* data have variable measurement durations, ranging from four months (sites 6 and 7) to about 16 months (sites 1 and 3). Time series of air temperature estimated for these sites on the basis of data from Dingri meteorological station may have biases due to climate change or shifts in weather patterns such as in the 1970s. Therefore, the estimated time series at higher elevations can only be considered as a first-order approximation.

Air temperatures have increased by 0.62 °C per decade over the last 49 years (1959–2007) at Dingri station (Fig. 9a). The warming rate exceeds the increase of the global mean air temperature over the last 50 years (0.13 ± 0.03 °C per decade; IPCC, 2007b), China as a whole during the period 1951–2001 (0.22 °C per decade; Ren et al., 2005), and the Tibetan Plateau during the periods 1955–1996 (0.16 °C per decade; Liu and Chen, 2000; Du et al., 2004; Frauenfeld et al., 2005) and 1960–2005 (0.25 °C per decade; You et al., 2010). The rate of air temperature increase at Dingri station is close to the warming rate in the source region of Yangtze river (5720 m a.s.l.; 0.5–1.1 °C per decade) (Kang et al., 2007) and in the southern Himalayan region (0.6–1.2 °C per decade) (Shrestha et al., 1999). This indicates that high elevations in this region are more sensitive to global warming than other regions at lower elevations. Such trends are also found in the European Alps (Diaz and Bradley, 1997), the tropics (Beniston et al., 1997) and other parts of the Tibetan Plateau (Tian et al., 2006). Similarly, such results, namely the higher the elevation the greater the warming, are also simulated with a nested regional climate model (Giorgi et al., 1997).

Seasonally, the greatest warming trend is observed in winter (December to February) with increasing trends of 0.86 °C per decade (Fig. 10d). These trends agree well with findings in the northern hemisphere (IPCC, 2007b), the Tibetan Plateau (Liu and Chen, 2000; Du et al., 2004; You et al., 2008; Zhang et al., 2006) and in the southern Himalayan region (Shrestha et al., 1999). The smallest warming trend occurs in summer (Fig. 10b).

Figure 9a shows annual anomalies of air temperature from 1959 to 2007 relative to 1971–2000 average mean annual air temperature. A cool period was evident during the 1960s, and somewhat warmer conditions have prevailed since about the mid-1980s. Only four relatively warm years with small anomalies of air temperature were recorded before the mid-1980s, whereas 17 warm years with large anomalies of air temperature have been recorded since the mid-1980s at Dingri. The last 10 years (1998 to 2007) rank among the warmest years since 1959; 2006 and 2007 were the warmest years with anomalies of 1.53 to 1.73 °C, followed by 1998 and 1999, with anomalies of 1.13 °C. In this respect, the record resembles that of China (Ren et al., 2005) and hemispheric-

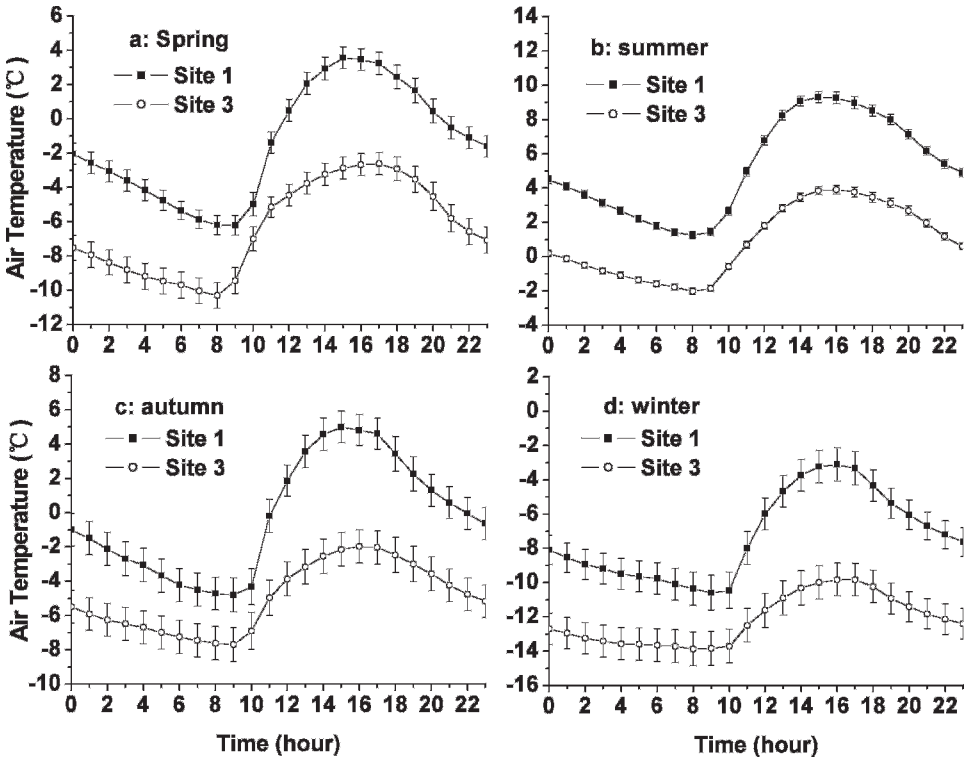

FIGURE 6. Mean diurnal variations of air temperatures in different seasons at sites 1 and 3 over period from May 2007 to August 2008. (a): Spring (March–May), (b): summer (June–August), (c): autumn (September–November); and (d): winter (December–February).

scale averages (IPCC, 2007b). Seasonally, there were a total of 3, 4, 6, and 8 warmer years (mean seasonal temperature above the 1971–2000 mean) before the mid-1980s, whereas a total of 19, 16, 14, and 15 warmer years occurred after the mid-1980s in spring, summer, autumn, and winter (Figs. 10a, 10b, 10c, and 10d). This means a warming trend occurred in all seasons after the mid-1980s and an accelerated warming trend appeared after 1998. Furthermore, anomalies of air temperature were larger in winter than in the other three seasons.

Many studies have found that glaciers in the Himalayan region and on the Tibetan Plateau as a whole have been retreating since the late 1960s (Yao et al., 2004; Thompson et al., 2006; Ye et al., 2006; Bolch et al., 2008; Kaspari et al., 2008). Based on ground measurements of terminus locations of the Rongbuk Glacier, it

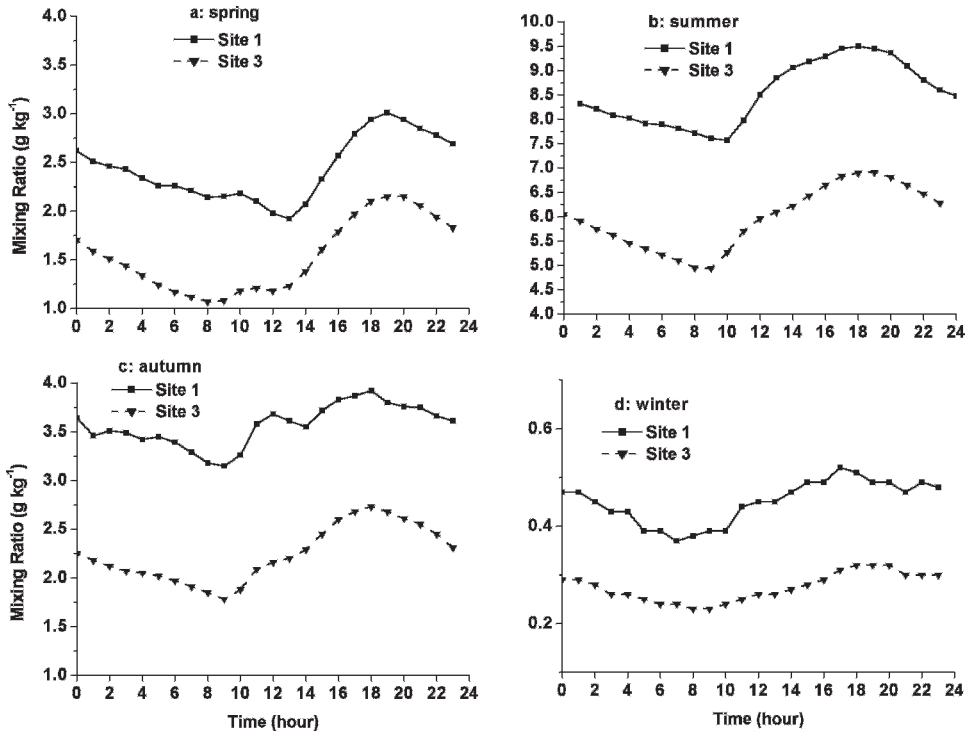

FIGURE 7. Mean diurnal variations of mixing ratio in different seasons at sites 1 and 3 over period from May 2007 to August 2008. Note that the scale of *y*-axis for summer (b) is two times of the scale for spring (a) and autumn (c) and 10 times of the scale for winter (d). (a): spring (March–May), (b): summer (June–August), (c): autumn (September–November); and (d): winter (December–February).

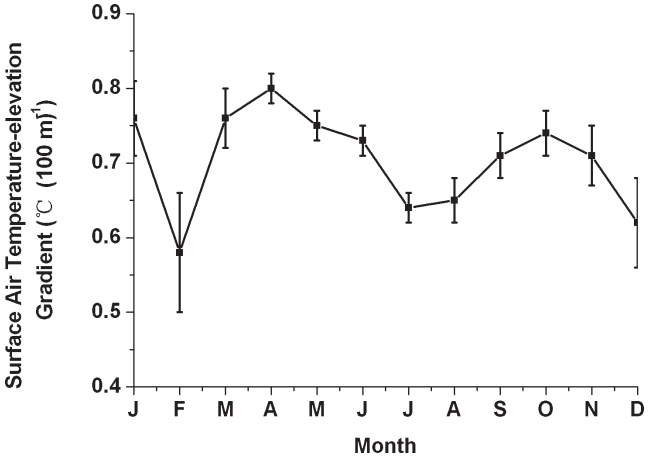

FIGURE 8. Monthly mean surface air temperature–elevation gradients on the north slope of Mt. Qomolangma. The mean values of surface air temperature–elevation gradients are calculated using data at all sites.

has been found that the retreat rate of the glacier terminus was about 5.5–8.7 m a^{-1} between 1966 and 1997 and 5.6–9.1 m a^{-1} between 1997 and 2001 (Ren et al., 2004). Using remote sensing and topographic data, Ye et al. (2009) calculated that the retreat rate of the Rongbuk Glacier's clean ice area increased from 0.31 km^2 a^{-1} between 1976 and 1992 to 0.48 km^2 a^{-1} between 1992 and 2003, with a weighted average retreat rate of about 0.38 km^2 a^{-1} from 1976 through 2003. The average thickness of the debris-covered glacier decreased about 24.2 m from 1974 through 2003, and the area of the supra-glacial lakes of the Rongbuk Glacier increased from about 0.13 km^2 in 1974 to about 0.79 km^2 in 1992. By 2003, the lake was completely decoupled from the glacier with an area of about 0.80 km^2.

It has been argued that the net snow accumulation on the north slope of Mt. Qomolangma region decreased rapidly during the 1950s and 1960s, but there has been no clear trend since the 1970s (Hou et al., 1999; Ren et al., 2004). Since there is no long-term precipitation record near the Rongbuk Glacier, precipitation records at Dingri are used to estimate its variation on the north slope of Mt. Qomolangma. The annual mean precipitation is about 263.2 ± 84.3 mm from 1959 to 2007. The long-term (1959–2007) seasonal mean precipitation ranges from about 8.4 ± 16.1 mm in spring, 223.1 ± 79.4 mm in summer, 29.7 ± 24.1 mm in autumn, to about 2.0 ± 3.3 mm in winter, respectively (Fig. 11). Summer precipitation accounts for about 85% of annual total precipitation, while variability of summer precipitation accounts for up to 94% of annual precipitation change. Summer precipitation also shows an increasing trend with a slope of 1.12 mm yr^{-1} and $p < 0.05$ (Fig. 11b), accounting for about 83% of the slope

TABLE 4

Linear correlation coefficients (R^2) of air temperature between each site and Dingri meteorological station (significant with $p < 0.05$). The coefficients between Dingri and site 1, 3, 4, 6, and 7 are calculated with mean daily air temperatures and the others based on hourly available air temperatures as shown in Table 1.

	Site 1	Site 3	Site 4	Site 6	Site 7
Dingri	0.88	0.86	0.85	0.58	0.15
Site 1	—	0.92	0.91	0.66	0.37
Site 3		—	0.90	0.84	0.42
Site 4			—	0.83	0.45

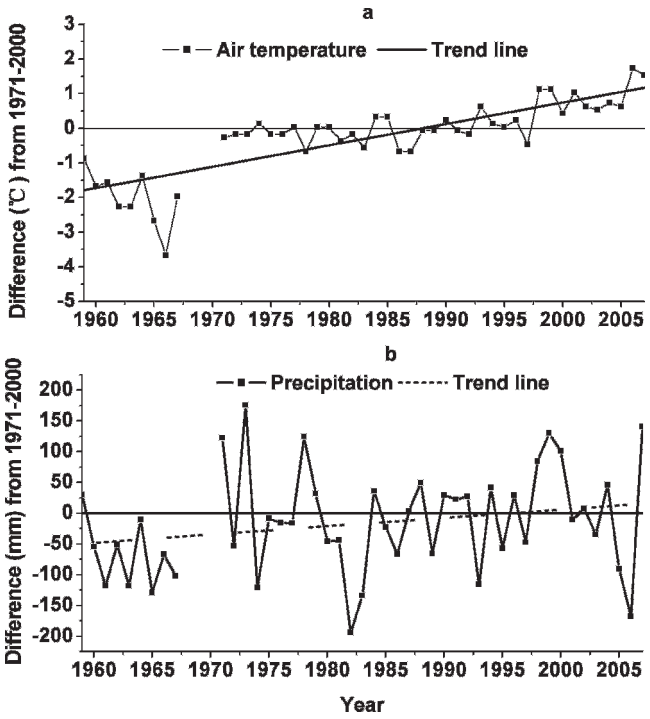

FIGURE 9. Anomalies of mean annual air temperature (a), and annual precipitation (b) from 1959 to 2007 at Dingri meteorological station. Both anomalies of mean annual air temperature and precipitation are calculated based on the 1971–2000 mean values.

(1.35 mm yr^{-1}) of annual precipitation increase (Fig. 9b). Further analysis indicates that precipitation has large inter-annual variability with no significant trend in the other seasons (Figs. 11a, 11c, and 11d). Therefore, change in summer precipitation dictates the annual trends. During the 1960s, precipitation was low (Fig. 9b) and a cooling trend was evident (Fig. 9a). This implied that reduction of precipitation was the main factor that caused a rapid decrease of net snow accumulation. Thereafter, precipitation shows an upward trend (Fig. 9b), especially in summer (Fig. 11b).

On the basis of the observed air temperature increase at Dingri station (Figs. 9a, 10a, 10b, 10c, 10d) and reported glacier retreat (Ren et al., 2004; Ye et al., 2009), we suggest that overall glacier retreat since the mid 1970s is probably mainly due to the increase in air temperature in the region. This is consistent with the conclusion reached by Thompson et al. (2006), that glacier retreat in the tropics and subtropics is caused by rising air temperature. However, it is highly possible that low precipitation during the 1960s may have caused less net snow accumulation, resulting in less ice moving to the ablation area and contributing to the rapid retreat of the Rongbuk Glacier since the mid 1970s. Further field measurements of ice velocity and glacier mass balance are critical for better understanding the changes in glaciers over the study area.

Discussion

Previous studies of stable isotopes in a few ice cores extracted from the north slope of the Himalaya (Hou et al., 1999; Qin et al., 2000; Thompson et al., 2000; Kang et al., 2001, 2007; Zhang et al., 2003) show that these stable isotopes could be used as an air temperature proxy, whereas others indicated a poor relationship between stable isotopes and air temperature due to a precipitation

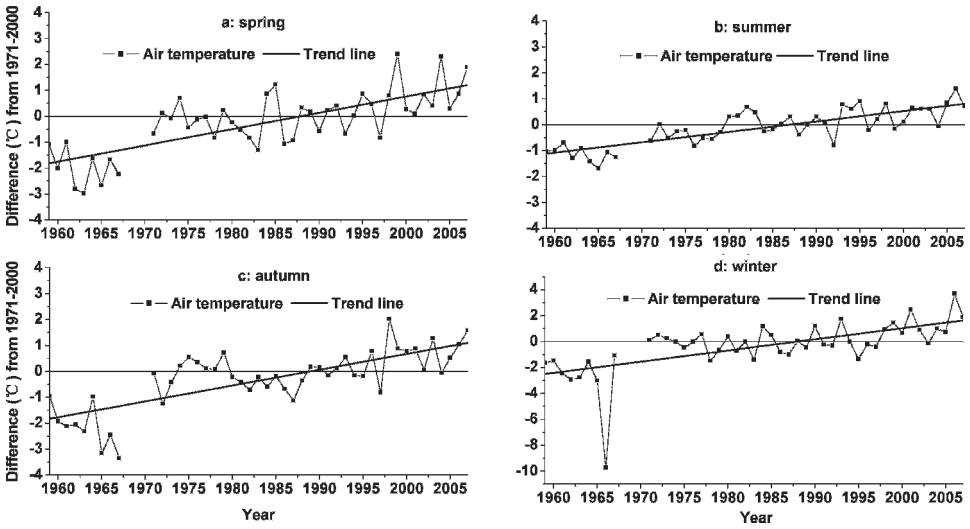

FIGURE 10. Anomalies of mean seasonal air temperature, relative to the 1971–2000 mean, from 1959 to 2007 at Dingri meteorological station. (a): Spring (March–May), (b): summer (June–August), (c): autumn (September–November); and (d): winter (December–February).

"amount effect" in the south Tibetan Plateau (Qin et al., 2000; Zhang et al., 2003). This effect causes a poor δ^{18}O-T relationship on both seasonal and annual scales (Tian et al., 2003). On the other hand, glacier ablation may occur in the accumulation region if the daily maximum air temperature is above 0 °C (see Fig. 3b). Moran and Marshall (2009) pointed out that meltwater percolation was the dominant process causing isotopic redistribution in Arctic snowpack during the melt season. Based on positive degree-day values, they suggested an average overestimation of 1.1 °C in average annual temperature reconstructions from the firn-core site (1727 m a.s.l.), located at the Prince of Wales Ice Field, Ellesmere Island, Canada, from 1967 to 2006. This may also strongly affect the chemical compositions of the snow and ice (Wagnon et al., 2003). Ice cores have been retrieved from the Mt. Qomolangma region, such as the East Rongbuk Glacier (Hou et al., 2002), the Far East Rongbuk Glacier (Kang et al., 2001), and Dasuopu Glacier (Thompson et al., 2000). Reconstructed climate and environmental changes from those ice core records show some significant differences (Kaspari et al., 2008), although physical locations of those ice cores are very close. It has been hypothesized that some *in situ* physical/chemical processes may be different, which may cause the differences in the reconstructed ice core records due to sublimation and ablation. Therefore it remains difficult to extract annual changes in air temperature from stable isotope records from Himalayan ice cores.

Summary

Hourly air temperature and relative humidity were recorded continuously over 16 months using seven automatic weather stations at elevations ranging from 5207 to 7028 m a.s.l. on the north slope of Mt. Qomolangma (Mt. Everest). The climate change and glacier's response are also analyzed using air temperature and precipitation time series (1959–2006) from the Dingri meteorological station. Results indicate that the vertical gradient in mean air temperature is non-linear due to the difference in surface between the moraine and ice field. Relative humidity does not change significantly with increasing elevation except on the ice field, but the mixing ratio decreases, especially from late May to early October when the area is under control of the southwesterly Indian monsoon. The mean diurnal range of air temperature decreases with increasing elevation and results in a diurnal range of relative humidity that also decreases with elevation. Maximum air temperature occurs significantly later at high elevation than at low elevation because the air temperature at high elevation is affected to a large extent by the downward mixing

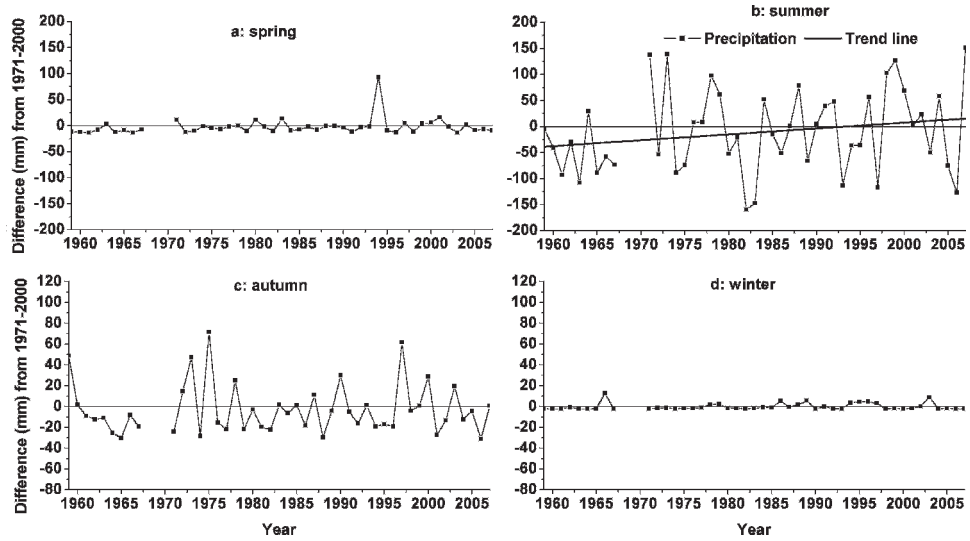

FIGURE 11. Anomalies of seasonal precipitation, relative to the 1971–2000 mean, from 1959 to 2007 at Dingri meteorological station. (a): Spring (March–May), (b): summer (June–August), (c): autumn (September–November); and (d): winter (December–February).

of warm air near the ablation zone of the glacier in the daytime. In contrast to the other sites where maximum relative humidity generally appears about daybreak, it occurs in the afternoon at site 6 due to the effect of convective clouds. The air moisture content reflects the pronounced alternation of the wet and dry seasons, and most water vapor is brought with the southwesterly Indian monsoon. The diurnal range of air temperature is smaller in summer than in spring because of the increased cloud cover. The annual mean surface air temperature-elevation gradients is 0.72 ± 0.01 °C $(100\ \text{m})^{-1}$, and shows a seasonal variation, being steeper in spring when conditions are dry and wind speeds are high, becoming shallow in summer when the north slope region of Mt. Qomolangma is under control of the southwesterly Indian monsoon.

Mean daily air temperatures from the Dingri meteorological station can be used to estimate long-term changes in air temperature on the north slope of Mt. Qomolangma. These data show a warming trend greater than that of global mean annual air temperature, and of mean annual air temperature in China as whole, and on the Tibetan Plateau, reflecting a more sensitive response to global warming in this high-elevation region. The greatest warming trend is observed in winter, and the smallest in summer. A cool period was evident during the 1960s, with warmer conditions prevalent since the mid-1980s, with a pronounced warming trend appearing after 1998. Reduced precipitation results in net snow accumulation decreasing rapidly during the 1960s, and a glacier retreat that may be caused by rising air temperature.

Acknowledgments

We would like to express our gratitude to the three anonymous reviewers for their insightful and constructive comments and inputs for the earlier manuscript. We thank B. Armstrong for English editing. We thank all the crew members during the field experiments, especially Wang Suichan, Zhang Zhigang, Du Wentao, and Sun Weijun, who implemented the glaciometeorological expedition to Mt. Qomolangma in 2007 and 2008. This work was in part supported by Chinese COPES project (GYHY200706005); National Basic Research Program of China (2007CB411503); and the International Arctic Research Center (IARC), University of Alaska Fairbanks, through the U.S. NSF cooperative agreement number OPP-0327664 to the University of Colorado at Boulder.

References Cited

Aizen, V. B., Aizen, E. M., Melack, J. M., and Dozier, J., 1997: Climatic and hydrologic changes in the Tian Shan, central Asia. *Journal of Climate*, 10: 1393–1404.

Barry, R. G., 1992: Mountain climatology and past and potential future climate changes in mountain regions: a review. *Mountain Research and Development*, 12: 71–86.

Barry, R. G., 2008: *Mountain Weather and Climate.* 3rd edition. Cambridge: Cambridge University Press.

Beniston, M., 2003: Climatic change in mountain regions: a review of possible impacts. *Climatic Change*, 59: 5–31.

Beniston, M., Diaz, H. F., and Bradley, R. S., 1997: Climatic change at high altitude sites: an overview. *Climatic Change*, 36: 233–251.

Bennett, M., 1997: Wind shear and the sea-breeze in Lincolnshire. *Weather*, 52: 198–203.

Bertolani, L., and Bollasina, M., 2000: Recent biennial variability of meteorological features in the eastern Highland Himalayas. *Geophysical Research Letters*, 27: 2185–2188.

Bolch, T., Buchroithner, M. F., Pieczonka, T., and Kunert, A., 2008: Planimetric and volumetric Glacier changes in Khumbu Himalaya since 1962 using Corona, Landsat TM and ASTER data. *Journal of Glaciology*, 54(187): 592–600.

Cai, X., Song, Y., Zhu, T., Lin, W., and Kang, L., 2007: Glacier winds in the Rongbuk Valley, north of Mount Everest: 2. their role in vertical exchange processes. *Journal of Geophysical Research*, 112: article D11102, doi:10.1029/2006JD007868.

Diaz, H. F., and Bradley, R. S., 1997: Temperature variations during the last century at high elevation sites. *Climatic Change*, 36: 253–279.

Du, M. Y., Kawashimaa, S., Yonemuraa, S., Zhang, X. Z., and Chen, S. B., 2004: Mutual influence between human activities and climate change in the Tibetan Plateau during recent years. *Global and Planetary Change*, 41: 241–249.

Duane, W. J., Pepin, N. C., Losleben, M. L., and Hardy, D. R., 2008: General characteristics of temperature and humidity variability on Kilimanjaro, Tanzania. *Arctic, Antarctic, and Alpine Research*, 40(2): 323–334.

Dyurgerov, M. D., and Meier, M. F., 2005: *Glaciers and the changing earth system: a 2004 snapshot*. Boulder, Colorado: Institute of Arctic and Alpine Research, University of Colorado, Occasional Paper 58, 117 pp.

Favier, V., Wagnon, P., Chazarin, J. P., Maisincho, L., and Coudrain, A., 2004: One-year measurements of surface heat budget on the ablation zone of Antizana Glacier 15, Ecuadorian Andes. *Journal of Geophysical Research*, 109: article D18105, doi:10.1029/2003JD004359.

Frauenfeld, O. W., Zhang, T., and Serreze, M. C., 2005: Climate change and variability using European Centre for Medium-Range Weather Forecasts reanalysis (ERA-40) temperatures on the Tibetan Plateau. *Journal of Geophysical Research*, 111: article D02101, doi:10.1029/2004JD005230, pp. 1–9.

Fujita, K., and Ageta, Y., 2000: Effect of summer accumulation on glacier mass balance on the Tibetan Plateau revealed by mass-balance model. *Journal of Glaciology*, 46(153): 244–252.

Gao, D., 1980: *Report on Scientific Expedition to Mt. Qomolangma Area (1975)—Meteorology and Environment*. Beijing: Science Press (in Chinese).

Giorgi, F., Hurrell, J. W., Marinucci, M. R., and Beniston, M., 1997: Elevation dependency of the surface climate signal: a model study. *Journal of Climate*, 10: 288–296.

Greuell, W., and Smeets, P., 2001: Variations with elevation in the surface energy on the Pasterze (Austria), *Journal of Geophysical Research*, 106(D23): 31717–31727.

Harding, R. J., 1979: Altitudinal gradients of temperatures in the northern Pennines. *Weather*, 34: 190–201.

Hou, S., Qin, D., Wake, C. P., and Mayewski, P. A., 1999: Abrupt decrease in recent snow accumulation at Mount Qomolangma (Everest), Himalaya. *Journal of Glaciology*, 45: 585–586.

Hou, S., Qin, D., Zhang, D., Ren, J., Kang, S., Mayewski, P. A., and Wake, C. P., 2002: Comparison of two ice core chemical records recovered from the Qomolangma (Mt. Everest) region. *Annals of Glaciology*, 35: 266–272.

IPCC, 2007a: Chapter 4. The physical science basis, changes in snow, ice and frozen ground. *In* Solomon, S., and Qin, D., et al. (eds.), *Contribution of Working Group I to the Fourth Assessment Report of IPCC*. New York: Cambridge University Press, 337–383.

IPCC, 2007b: Chapter 3. The physical science basis, surface and atmospheric climate change. *In* Solomon, S., and Qin, D., et al. (eds.), *Contribution of Working Group I to the Fourth Assessment Report of IPCC*. New York: Cambridge University Press, 235–336.

Jenkins, M. D., Drever, J. I., and Reider, R. G., 1987: Chemical composition of fresh snow on Mount Everest. *Journal of Geophysical Research*, 92(D9): 10999–11002.

Kang, S., Qin, D., Mayewski, P. A., Wake, C. P., and Ren, J., 2001: Climatic and environmental records from the Far East Rongbuk ice core, Mt. Qomolangma (Everest). *Episodes*, 24(3): 176–181.

Kang, S., Zhang, Y., Qin, D., Ren, J., Zhang, Q., Grigholm, B., and Mayewski, P. A., 2007: Recent temperature increase recorded in an ice core in the source region of Yangtze River. *Chinese Science Bulletin*, 52(6): 825–831.

Kaser, G., Cogley, J. G., Dyurgerov, M. B., Meier, M. F., and Ohmura, A., 2006: Mass balance of glaciers and ice caps: consensus estimates for 1961–2004. *Geophysical Research Letters*, 33: doi:10.1029/2006GL027511.

Kaspari, S., Hooke, L. R., Mayewski, P. A., Kang, S., Hou, S., and Qin, D., 2008: Snow accumulation rate on Qomolangma (Mount Everest), Himalaya: synchroneity with sites across the Tibetan Plateau on 50–100 year timescales. *Journal of Glaciology*, 54: 343–352.

Liu, X., and Chen, B., 2000: Climatic warming in the Tibetan Plateau during recent decades. *International Journal of Climatology*, 20: 1729–1742.

Meier, M. F., Dyurgerov, M. B., Rick, U. K., O'Neel, S., Pfeffer, W. T., Anderson, R. S., Anderson, S. P., and Glazovsky, A. F., 2007: Glaciers dominate eustatic sea-level rise in the 21st century. *Science*, 317: 1064–1067.

Moore, G. W. K., and Semple, J. L., 2004: High Himalayan meteorology: weather at the South Col of Mount Everest. *Geophysical Research Letters*, 31: doi:10.1029/2004GL020621.

Moran, T., and Marshall, S., 2009: The effects of meltwater percolation on the seasonal isotopic signals in an Arctic snowpack. *Journal of Glaciology*, 55: 1012–1024.

Oerlemans, J., and Vugts, H. F., 1993: A meteorological experiment in the melting zone of the Greenland ice sheet. *Bulletin of the American Meteorological Society*, 74(3): 355–365.

Pepin, N. C., 2000: Twentieth-century change in the climate record for the Front Range, Colorado, U.S.A. *Arctic, Antarctic, and Alpine Research*, 32: 135–146.

Pepin, N. C., 2001: Surface air temperature-elevation gradients changes in northern England. *Theoretical and Applied Climatology*, 68: 1–16.

Qin, D., 1999: *Map of Glacier Resources in the Himalayas*. Beijing: Science Press, Scale 1: 500, 000, sheet 7.

Qin, D., Mayewski, P. A., Wake, C. P., Kang, S., Ren, J., Hou, S., Yao, T., Yang, Q., Jing, Z., and Mi, D., 2000: Evidence for recent climate change from ice cores in the central Himalaya. *Annals of Glaciology*, 31: 153–158.

Raper, S. C. B., and Braithwaite, R. J., 2006: Low sea level rise projections from mountain glaciers and icecaps under global warming. *Nature*, 439: 311–313.

Rees, H. G., and Collins, D. N., 2006: Regional differences in response of flow in glacier-fed Himalayan rivers to climate warming. *Hydrological Processes*, 20: 2157–2167.

Reijmer, C. H., and Oerlemans, J., 2002: Temporal and spatial variability of the surface energy balance in Dronning Maud Land, East Antarctica, *Journal of Geophysical Research*, 107(D24), doi:10.1029/2000JD000110.

Ren, G. Y., Guo, J., Xu, M. Z., Chu, Z. Y., Zhang, L., Zou, X. K., Li, Q. X., and Liu, X. N., 2005: Climate changes of mainland China over the past half century. *Acta Meteorologica Sinica*, 63(6): 942–955, (in Chinese).

Ren, J., Qin, D., Kang, S., Hou, S., Pu, J., and Jin, Z., 2004: Glacier variations and climate warming and drying in the central Himalayas. *China Science Bulletin*, 49: 65–69.

Richardson, A. D., Lee, X., and Friedland, A. J., 2004: Microclimatology of treeline spruce-fir forests in mountains of the northeastern United States. *Agricultural and Forest Meteorology*, 125: 53–66.

Rolland, C., 2003: Spatial and seasonal variations of air temperature surface air temperature–elevation gradients in Alpine regions. *Journal of Climate*, 16: 1032–1046.

Schneider, C., 1999: Energy balance estimates during the summer season of glaciers of the Antarctic Peninsula. *Global and Planetary Change*, 22: 117–130.

Shen, Z., 1975: *The Scientific Investigation Report on Mt. Qomolangma Region (1966–1968)—Meteorology and Solar Radiation*. Beijing: Scientific Press (in Chinese).

Shi, Y., 2004: *Chinese Glacier Inventory*. Beijing: Scientific Press (in Chinese).

Shi, Y., 2008: *Collectanea of the Studies on Glaciology, Climate and Environmental Changes in China*. Beijing: China Meteorological Press.

Shrestha, A. B., Wake, C. P., Mayewski, P. A., and Dibb, J. E., 1999: Maximum temperature trends in the Himalaya and its vicinity: an analysis based on temperature records from Nepal for the period 1971–94. *Journal of Climate*, 12: 2775–2786.

Sicart, J. E., Wagnon, P., and Ribstein, P., 2005: Atmospheric controls of the heat balance of Zongo Glacier (16°S, Bolivia). *Journal of Geophysical Research*, 110: article D12106, doi:10.1029/2004JD005732.

Somervell, T. H., and Whipple, F. J. W., 1926: The meteorological results of the Mount Everest expedition. *Quarterly Journal of the Royal Meteorological Society*, 52: 131–144.

Tang, Z., and Fang, J., 2006: Temperature variation along the northern and southern slopes of Mt. Taibai, China. *Agricultural and Forest Meteorology*, 139: 200–207.

Thompson, L. G., Yao, T., Davis, M. E., Henderson, K. A., and Lin, P. N., 2000: A high-resolution millennial record of the South Asian Monsoon from Himalayan ice cores. *Science*, 289: 1916–1919.

Thompson, L. G., Mosley-Thompson, E., Brecher, H., Davis, M., León, B., Les, D., Lin, P., Mashiotta, T., and Mountain, K., 2006: Abrupt tropical climate change: past and present. *Proceedings of the National Academy of Sciences of the U.S.A.*, 103(28): 10536–10543.

Tian, L., Yao, T., Schuster, P. F., White, J. W. C., Ichiyanagi, K., Pendall, E., Pu, J., and Yu, W., 2003: Oxygen-18 concentrations in recent precipitation and ice cores on the Tibetan Plateau. *Journal of Geophysical Research*, 108(D9): 4293, doi:10.1029/2002JD002173.

Tian, L., Yao, T., Li, Z., MacClune, K., Wu, G., Xu, B., Li, Y., Lu, A., and Shen, Y., 2006: Recent rapid warming trend revealed from the isotopic record in Muztagata ice core, eastern Pamirs. *Journal of Geophysical Research*, 111: article D13103, doi:10.1029/2005JD006249.

Wagnon, P., Ribstein, P., Francou, B., and Pouyaud, B., 1999: Annual cycle of energy balance of Zongo Glacier, Cordillera Real, Bolivia. *Journal of Geophysical Research*, 104(D4): 3907–3923.

Wagnon, P., Sicart, J. E., Berthier, E., and Chazarin, J. P., 2003: Wintertime high-latitude surface energy balance of a Bolivian glacier, Illimani, 6340 m above sea level. *Journal of Geophysical Research*, 108(D6), doi:10.1029/2002JD002008.

Xie, Z., 1975: *The Scientific Investigation Report on Mt. Qomolangma Region (1966–1968)—Modern Glaciers and Physiognomy*. Beijing: Scientific Press (in Chinese).

Yanai, M., and Li, C., 1994: Mechanism of heating and the boundary layer over the Tibetan Plateau. *Monthly Weather Review*, 122: 305–323.

Yang, X. G., Zhang, T. J., and Qin, D. H., et al. (2010). Diurnal and seasonal characteristics of wind field on the north slope of Mt. Qomolangma (Mt. Everest). *Monthly Weather Review*. (under review).

Yao, T. D., Wang, Y. Q., Liu, S. Y., Pu, J. C., Shen, Y. P., and Lu, A. X., 2004: Recent glacial retreat in High Asia in China and its impact on water resource in Northwest China. *Science China D*, 47(12): 1065–1075.

Ye, D., and Gao, Y., 1979: *Meteorology of the Tibetan Plateau*. Beijing: Science Press, 278, (in Chinese).

Ye, Q., Kang, S., Feng, C., and Wang, J., 2006: Monitoring glacier variations on Geladandong mountain, central Tibetan Plateau, from 1969 to 2002 using remote-sensing and GIS technologies. *Journal of Glaciology*, 52(179): 537–545.

Ye, Q., Zhong, Z., Kang, S., Stein, A., Wei, Q., and Liu, J., 2009: Monitoring glacier and supra-glacier lakes from space in Mt. Qomolangma region of the Himalayas on the Tibetan Plateau in

China. *Journal of Mountain Sciences*, 6(6): 101–106, doi:10.1007/s11629-009-1025-3.

You, Q., Kang, S., Pepin, N. C., Flügel, W., Yan, Y., Behrawan, H., and Huang, J., 2010: Relationship between temperature trend magnitude, elevation and mean temperature in the Tibetan Plateau from homogenized surface stations and reanalysis data. *Global and Planetary Change*, 71: 124–133.

You, Q., Kang, S., Aguilar, E., and Yan, Y., 2008: Changes in daily climate extremes in the eastern and central Tibetan Plateau during 1961–2005. *Journal of Geophysical Research*, 113: article D07101, doi:10.1029/2007JD009389.

Zhang, D., Qin, D., Hou, S., Ren, J., Mayewski, P. A., and Kang, S., 2003: The climatic meaning of $\delta^{18}O$ in the East Rongbuk 80.36 m depth ice-core, Mt. Qomolangma. *Science China D*, 33: 264–270, (in Chinese).

Zhang, Q., Kang, S., and Yan, Y., 2006: Characteristics of spatial and temporal variations of monthly mean surface air temperature over Qinghai-Tibet Plateau. *Chinese Geographical Science*, 16(4): 351–358.

Zhang, T., Osterkamp, T. E., and Stamnes, K., 1996: Some characteristics of the climate in northern Alaska, U.S.A. *Arctic and Alpine Research*, 28: 509–518.

Zhang, T., 2007: Perspectives on environmental study of response to climatic and land cover/land use change over the Qinghai-Tibetan Plateau: an introduction. *Arctic, Antarctic, and Alpine Research*, 39: 631–634.

Zou, H., Zhou, L., Ma, S., Li, P., Wang, W., Li, A., Jia, J., and Gao, D., 2008: Local wind system in the Rongbuk Valley on the northern slope of Mt. Everest. *Geophysical Research Letters*, 35: article L13813, doi:10.1029/2008GL033466.